Constitutional Isomeric Effect on the Dielectric Relaxation of a Nematic Liquid Crystalline Polymethacrylate Containing a Methoxymethylstilbene Side Group

Z. Z. Zhong,* D. E. Schuele, S. W. Smith, and W. L. Gordon

Department of Physics, Case Western Reserve University, Cleveland, Ohio 44106-7079

Received December 29, 1992; Revised Manuscript Received July 20, 1993®

ABSTRACT: Broad band frequency (0.1 Hz–10 MHz) dielectric relaxation spectroscopy has been utilized to investigate nematic liquid crystalline polymethacrylates containing a constitutional isomeric methoxymethylstilbene mesogen in the side chain (4-6-PMA and 4′-6-PMA). While 4-6-PMA shows two typical relaxation processes in a side-chain liquid crystalline polymer system, 4′-6-PMA essentially has one relaxation process. The temperature-dependent relaxation times, obtained through Havriliak–Negami data fitting, show "kinks" near calorimetric nematic–isotropic transition and a non-Arrhenius characteristic toward the glass transition. The glass behavior has been fitted with a Vogel–Fulcher–Tammann–Hesse (VFTH) equation and a general formula for activation energy has been derived in terms of VFTH parameters.

Introduction

During the past two decades, polymers exhibiting a liquid crystalline state have become of theoretical and technological interest because of their properties, which are a combination of polymer-specific properties and the anisotropic behavior of liquid crystals.[1-6] Side-chain liquid crystalline polymers (LCP's) are polymers that have linked conventional low molecular mass liquid crystal (LC's) as side chains to a polymer backbone through a flexible spacer (usually a methylenic group $-CH_2-$). The nature of the mesomorphic phases exhibited by side-chain LCP's with degrees of polymerization higher than 12 are usually controlled by the spacer length and the nature of the mesogenic group. For the same spacer length and the degree of polymerization, the degree of decoupling the mesogenic side group from the polymer backbone seems to be strongly correlated to the nature of the polymer backbone.[7-11]

Percec and co-workers have suggested that side-chain liquid crystalline "copolymers" of the monomer pairs containing constitutional isomeric mesogenic units are useful both to depress side-chain crystallization of polymers containing long flexible spacers and to obtain qualitative information about the degree of decoupling.[8] In the synthesis and characterization of copolymethacrylate and copolyacrylate based on side groups with two isomeric methoxymethylstilbenes,[7] they found a suppression of side-chain crystalline and transformation of monotropic mesophases into enantiotropic mesophases by copolymerization of the parent polymers' monomer pairs containing constitutional isomeric mesogenic side groups. Copolymers of constitutional isomeric groups may represent a chemical sensor which provides at least qualitative information on the dynamics of the side-chain LCP's. Therefore, it is of interest to investigate comparatively the corresponding homopolymers with the same constitutional isomeric mesogen in the side group. Silvestri and Koenig employed ^{13}C nuclear magnetic resonance (NMR) spectroscopy to study the local molecular dynamics of polymethacrylate attached to a 4-hydroxy-4′-methoxy-α-methylstilbene side chain through a methylenic spacer length of three (4′-3-PMA).[12] Within the glassy state, the mobility of all spins increased continuously with temperature due to thermal motions. The mobility then increased discontinuously at the glass to mesogenic phase transition. They observed that the outer carbons in the spacer are nearly as rigid as the mesogen while the center spacer carbon is nearly 2 orders of magnitude more mobile. Gu and Jamieson *et al.* attempted dynamic light scattering from a nematic monodomain containing polymethacrylate with 4-methoxy-4′-hydroxy-α-methylstilbene side group linked by a spacer length of six (4-6-PMA).[13] The addition of the side-chain LCP to a nematic LC (4′-*n*-pentyl-4-cyanobiphenyl, or 5CB) results in significant increases in the relaxation times from all three scattering geometries (splay, bend, and twist), which had been attributed to small decreases of the three elastic constants and larger increases of the three viscosities.

In this paper, we will report and discuss the dielectric results of two liquid crystalline polymethacrylates containing a constitutional isomeric methoxymethylstilbene side group (4-6-PMA and 4′-6-PMA) within the same side-chain LCP series mentioned above. The dielectric relaxation spectroscopy with broad frequency band (10^{-1}–10^7 Hz) shows that there are two typical relaxation processes in the nematic phase for 4-6-PMA and there is basically only one process for 4′-6-PMA. The results will be interpreted in terms of rotational dynamic theory in liquid crystals[14-18] and Vogel–Fulcher–Tammann–Hesse (VFTH) glassy diagram.[19-21]

Experimental Section

The two thermotropic liquid crystalline polymethacrylates with a constitutional isomeric mesogens in the side chain were synthesized by Percec and co-workers using radical polymerization of monomers, one containing 4-methoxy-4′-hydroxy-α-methylstilbene (4-6-PMA)[9] and another containing 4-hydroxy-4′-methoxy-α-methylstilbene (4′-6-PMA).[8] The molecular structure is shown in Chart I, which contains an isomeric methoxymethylstilbene attached to a polymethacrylate backbone via a flexible methylenic spacer length of six. The isomerism was determined by the position of methyl unit ($-CH_3$) in the bridging group of methylstilbene.

Molecular weight was determined by gel permeation chromatography (GPC).[8] Both samples are in a nematic state at a temperature slightly higher than room temperature, verified by a Nikon polarizing microscope with a custom-built hot stage. Differential scanning calorimetric (DSC) measurements were taken with a DuPont 910 cell base incorporating a DuPont 990 thermal analyzer at a 10 K/min heating rate. The mesogenic phase transitions were recorded at the maximum or minimum

® Abstract published in *Advance ACS Abstracts,* October 15, 1993.

0024-9297/93/2226-6403$04.00/0

Chart I. Molecular Structure for the Studied Side-Chain Liquid Crystalline Polymethacrylate (LCP) Containing either 4-Methoxy-4'-hydroxy-α-methylstilbene (4-6-PMA) or 4-Hydroxy-4'-methoxy-α-methylstilbene (4'-6-PMA)[a]

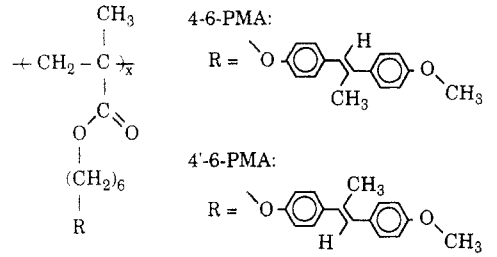

[a] The *trans* conformational molecule of the mesogenic side chain is presented as drawn.

Table I. Phase Transitions of 4-6-PMA and 4'-6-PMA from the Repeated DSC Scan at 10 K/min Heating Rate (g, glass; n, nematic; i, isotropic)

polymer	name	$10^{-3}\bar{M}_n$	$\bar{M}_w/\bar{M}_n$	DP ($\bar{x}$)	phase transitions (K)
I	4-6-PMA	11.63	1.36	29	g 302 n 387 i
II	4'-6-PMA	24.70	2.50	60	g 302 n 372 i

of their endothermic peaks while glass transition temperatures (T_g) were recorded at the midpoint of the step change in the heat capacity. Each sample was measured at least 3 times. Table I summarizes the number-average molecular weight (M_n), the width of molecular-weight distribution (M_w/M_n), the degree of polymerization (DP), and phase transitions from the repeated heating scans.

Four capacitance bridges were employed in the dielectric measurement in order to obtain the permittivity (ϵ') and loss factor (ϵ'') over a broad frequency range: TA DEA 2970 dielectric analyzer (0.1 Hz–100 kHz), HP 4284A Precision LCR Meter (20 Hz–1 MHz), HP 4275A multifrequency LCR meter (20 kHz–10 MHz), and CGA-83 ratio-arm transformer bridge (10 Hz–100 kHz).[22]

The low-frequency measurements were completed with DEA 2970 which employed parallel ceramic plates with gold-coated three-terminal sensors,[23] separated by a 50-μm Kapton spacer. The sample was first applied to the center of the bottom sensor and heated to melt at about 450 K for 10 min. The upper sensor was driven into the sample with a 150-N force to reach the final 50-μm separation. The DEA was programmed to measure dielectric permittivity (ϵ') and loss factor (ϵ'') isothermally at 2.5 K temperature increments from 300 to 430 K, over a frequency range from 0.1 Hz–100 kHz at four frequencies per decade with the excitation voltage being approximately 1 V.

For the measurements with the other bridges, the dielectric sample cell was constructed of two parallel ITO (indium–tin–oxide, 20 Ω/□) glass plates, which allows for optical examination. The edge of the ITO plate was stripped using a solution of hydrochloric and nitric acids. The two plates, separated by a 25-μm Kapton spacer, were adhered together with a high temperature epoxy to form a parallel-plate capacitor with the empty cell capacitance C_0 of approximately 10 pF. The sample 4-6-PMA was inserted onto the cell through capillary action, being placed on a hot stage in a vacuum chamber and heated above the isotropic temperature. The sample 4'-6-PMA having a much higher viscosity was first applied to one ITO glass plate heated to well above its isotropic point; the top ITO plate was then pressed and squeezed onto the sample, followed by slowly cooling down to room temperature under a constant force. This sample cell was completed by sealing with a high temperature epoxy. Each sample cell was placed in a custom-built vacuum oven for data collection at elevated temperatures from 300–400 K. The temperature was controlled by a Lakeshore DRC 82C controller with two platinum thermal sensors, which can stabilize temperature to within 10 mK. The data acqusition steps were controlled by a HP-87 computer through an IEEE-488 bus interface.

All the data have been converted to permittivity ϵ' and loss factor ϵ'' (complex dielectric constant $\epsilon^*(\omega) = \epsilon'(\omega) - i\epsilon''(\omega)$) through the simple relations $\epsilon'(\omega) = C(\omega)/C_0$ and $\epsilon''(\omega) = (G/\omega)/C_0$, where $C(\omega)$ is the loaded capacitance and $G(\omega)/\omega$ is the dielectric loss, equal to the product of dissipative factor $D(\omega)$ or $\tan\delta(\omega)$ and capacitance $C(\omega)$. At the frequency 10 kHz and temperature 300 K, the dielectric constant ϵ' and conductivity $\sigma(=\epsilon''\epsilon_0\omega)$ of the sample 4-6-PMA are typically measured to be 3.16 and 2.20×10^{-9} S/m, respectively, while the values are 3.60 and 1.75×10^{-9} S/m for 4'-6-PMA.

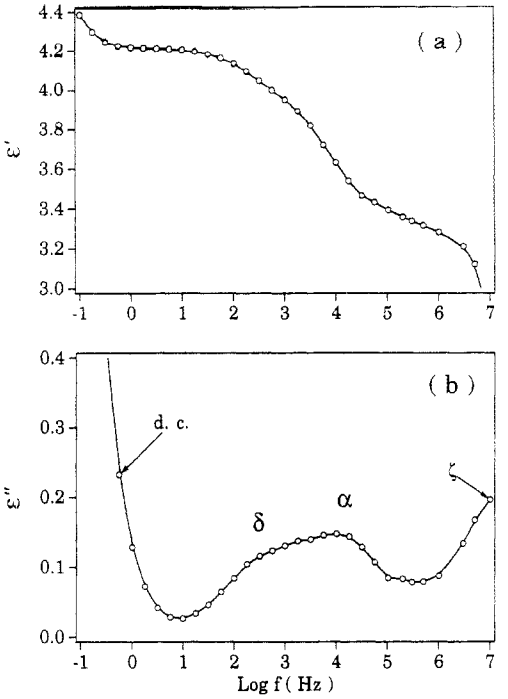

Figure 1. Dielectric spectrum overview of the nematic side-chain LCP 4-6-PMA at 350.14 K, which consists of four components in the measured frequency range (0.1 Hz–10 MHz), a dc conductivity, two major relaxation processes (α and δ) of the mesogens in the side chain, and a ζ process at the high frequency end: (a) permittivity ϵ'; (b) loss factor ϵ'' of the complex dielectric constant ϵ^*.

Results and Discussion

Figure 1 shows the dielectric spectroscopy of the 4-6-PMA in the nematic phase at 350.14 K. Either the real part $\epsilon'(\omega)$ or the imaginary part $\epsilon''(\omega)$ of the complex dielectric constant $\epsilon^*(\omega)$ provides complete information regarding all the processes as a result of the Kramers–Kronig relations. In the frequency range from 0.1 Hz to 10 MHz, the dielectric spectrum shows dc conductivity, two major relaxation processes of the mesogen in the side chain—labeled by the low-frequency δ and the high-frequency α, and a not-so-clear ζ process at the high frequency end. This kind of loss peak labeling (δ, α with decreasing temperature) is contrary to the traditional nomenclature for polymeric materials (α, β, γ, ... with decreasing temperature), but has been widely accepted by authors in the LCP field.[24–27] The ζ process which exhibits no temperature dependence of the peak position might result from two possibilities. One is the "localized" β relaxation, which is often observed with low intensity but appears to be at the extremely high frequency end when the temperature goes above T_g. The other is due to the surface resistivity of the ITO glass. The possibility of the β relaxation can be ruled out since the amplitudes of the ζ process are higher than those of the δ- and α-processes at $T > 330$ K and the ζ process, with temperature-independence of maximum frequency position, contains no molecular relaxation mechanism. By measurement of the empty cell, the effective surface resistance is approximately 50 Ω at 5 MHz and 350 K, and the loaded

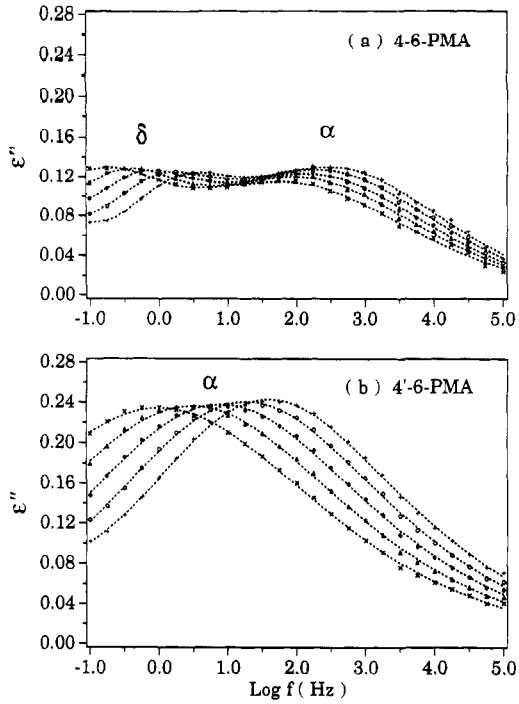

Figure 2. Dielectric relaxation spectra obtained by DEA 2790 from 315 to 325 K: ×, 315.15 K; △, 317.65 K; ◇, 320.15 K; ○, 322.65 K; +, 325.15 K; (a) 4-6-PMA; (b) 4'-6-PMA. Both samples endured the strictly same measuring procedures. Dashed curves are the least-squares fitting according to the Havriliak–Negami equation (4) plus a dc conductivity equation (1).

capacitance is approximately 40 pF. So, $f \sim (2\pi RC)^{-1} \sim 8.0 \times 10^7$ Hz, which is very close to the extrapolated frequency of the ζ process. Thus the ζ process is thought to be due to the ITO cell resistance and will not be included.[28] In the following, we shall only focus on the two major relaxation processes α and δ of the mesogens of the side-chain LCP.

Havriliak–Negami Data Fitting. Figure 2 shows the dielectric relaxation spectra (0.1 Hz–100 kHz) in the temperature range from 315 to 325 K. Figure 2a for 4-6-PMA has both δ and α processes while Figure 2b for 4'-6-PMA has only an α process. The data have been fitted with Havriliak–Negami (HN)[29] empirical line shapes plus a dc conductivity using a least-squares method. Usually, the dc conductance component obeys a power rule of frequency $\omega(=2\pi f)$; here we simply treat it as a pure dc conductivity, i.e.

$$\epsilon_{dc}'' = \sigma_{dc}/\epsilon_0\omega \tag{1}$$

The Havriliak–Negami function is

$$\frac{\epsilon^*(\omega) - \epsilon_\infty}{\epsilon_0 - \epsilon_\infty} = \frac{1}{[1 + (i\omega\tau)^{1-\gamma}]^\beta} \tag{2}$$

where ϵ_0 and ϵ_∞ are the limiting low- and high-frequency permittivities, respectively, $\Delta\epsilon \equiv \epsilon_0 - \epsilon_\infty$ is the dielectric relaxation strength, representing the effective dipole moment of the orienting unit; τ is a relaxation time, $\tau = (2\pi f_R)^{-1}$, where f_R is a relaxation frequency; parameter $\gamma(0 \le \gamma \le 1)$ describes the symmetric width of relaxation time distribution, and the width increases as γ ranges from 0 to 1; and parameter $\beta(0 < \beta \le 1)$ describes the skewness of the relaxation time distribution, and the skewness increases as β ranges from 1 to 0. When $\beta = 1$ a Cole–Cole[30] circular arc is obtained, when $\gamma = 0$ a Cole–Davidson[31] skewed semicircle is obtained, and when $\beta = 1$ and $\gamma = 0$ a Debye[32] relaxation function is obtained.

Equation 2 can be separated into the real and imaginary parts

$$\epsilon'(\omega) - \epsilon_\infty = r^{-\beta/2}\,\Delta\epsilon \cos\beta\theta \tag{3}$$

$$\epsilon''(\omega) = r^{-\beta/2}\,\Delta\epsilon \sin\beta\theta \tag{4}$$

with

$$r = \left[1 + (\omega\tau)^{1-\gamma}\sin\left(\frac{\pi}{2}\gamma\right)\right]^2 + \left[(\omega\tau)^{1-\gamma}\cos\left(\frac{\pi}{2}\gamma\right)\right]^2 \tag{5}$$

$$\theta = \arctan\left[\frac{(\omega\tau)^{1-\gamma}\cos\left(\frac{\pi}{2}\gamma\right)}{1 + (\omega\tau)^{1-\gamma}\sin\left(\frac{\pi}{2}\gamma\right)}\right] \tag{6}$$

Figure 2 also demonstrates the HN least-squares fitting results (dashed curves) according to eq 4 in the temperature range 315–325 K. This data fitting has been applied to both isomeric samples from nematic phase to isotropic phase (300–400 K) to obtain the necessary information about each relaxation process, such as relaxation time τ, dielectric relaxation strength $\Delta\epsilon$, etc.

Table II gives an example of the HN fitting results at 325.15 K. The dc conductivity σ_{dc} for 4-6-PMA is 1.6×10^{-13} S/m and larger than that of 4'-6-PMA, 4.0×10^{-14} S/m. For 4-6-PMA, the data were fitted with two HN loss factors according to eq 4 by first extracting a dc conductance (eq 1). The relaxation strength $\Delta\epsilon$ of the δ process is 0.27, smaller than that of the α process, 0.74. This difference can be attributed to the smaller longitudinal dipole moment μ_l of the mesogen in the side chain which is essentially associated with the δ peak and the larger transverse component μ_t which is mainly associated with the α peak.[15,24,27,33] The width parameter of the δ peak ($\gamma = 0.33$) is narrower than that of the α peak ($\gamma = 0.59$). Both processes have the skewness parameter β slightly larger than 1, and we set $\beta = 1.0$ (see Table II), which indicates the HN function has been reduced to a Cole–Cole expression. The data for 4'-6-PMA were fitted into one HN loss factor $\epsilon''(\omega)$ (eq 4) plus a dc conductance (eq 1) with the dielectric strength $\Delta\epsilon$ of 1.84, $\gamma = 0.64$, and $\beta = 0.79$. The relaxation time of 4'-6-PMA, $\tau = 7.78 \times 10^{-3}$ s, is between the two relaxation times of 4-6-PMA, 3.52×10^{-4} s (α peak) and 9.19×10^{-2} s (δ peak).

Isomeric Effect on Two Major Relaxations—α and δ. The two major relaxation processes in mesogenic phase of a side-chain LCP are often interpreted in terms of the rotational dynamic theory in liquid crystals.[14,15,17,24,27,34] Generally speaking, they arise from the reorientations of the mesogens in the side chain. In a uniaxial liquid crystal system, the dipole moment of a mesogen can be divided into a longitudinal component μ_l (usually along the long axis of the molecule, sometimes equal to the easy optical axis) and a transverse component μ_t (usually perpendicular to the long axis of the molecule). The low-frequency δ peak can be assigned to the "rotation" of the longitudinal dipole moment in the mesogenic group about its short axis. However, it does not need to be strictly a simple rotation about the short axis. Any significant change of the polar angle with the laboratory frame should contribute to this δ process.[17,35] In the studied side-chain LCP system, pure rotation about the short axis is topologically restricted. There is however, a possibility of a large scale reorientation of the long axis of the mesogenic unit, but only together with the spacer. Such a process may also involve a section of the backbone chain. The high-frequency α peak, meanwhile, can be thought to involve both longitudinal and transverse dipole moments in the mesogenic group, combined into a few different rotational

Table II. Results from Havriliak-Negami Data Fittings at 325.15 K after Extracting a dc Factor Equation (1)

		δ process				α process			
sample	σ_{dc} (10^{-12} S/m)	$\Delta\epsilon$	τ (s)	γ	β	$\Delta\epsilon$	τ (s)	γ	β
4-6-PMA	0.16	0.27	9.19 ± 10^{-2}	0.33	1.0	0.74	3.52×10^{-4}	0.59	1.0
4′-6-PMA	0.04					1.84	7.87×10^{-3}	0.64	0.79

modes. The major contribution to the α process comes from the transverse dipole moment μ_t rotating about the mesogen's long axis.

It is worth pointing out here that the above interpretation, based on the general rotational dynamic theory,[17,35] is in qualitative agreement with the processes in polymeric liquid crystals. The theory only requires that the conditional probability distribution function be expanded in terms of correlation functions of the motion, which are not specific to any rotational (diffusion) model.[18,36] In side chain polymeric liquid crystal materials, steric hindrance prevents a simple reorientation of the side chain mesogenic unit about its long or short axes. Reorientations of the unit, if any, are possible only as a result of highly cooperative motions involving both rotation and translation of the unit and of the neighboring environment.

Kresse and co-workers made dielectric relaxation measurements on two isomeric siloxane polymers with opposite direction of the ester bridging group in the phenylbenzoate mesogenic side group.[37] The ratio of the amplitudes of the two major relaxation processes in the mesogenic phase is strongly correlated to the isomerism, which can be simply attributed to the different ratios of longitudinal and transverse components of dipole moments for the side group. The dipole moment in the constitutional isomeric mesogen of the side-chain LCP in this paper mainly comes from the two polar heads, consisting of the phenyl–O–CH_3 bond at two ends of methylstilbene molecule and each carrying about 1.28 D, as well as from the bridging group in the stilbene effectively carrying a longitudinal dipolar component.[38-40] The stilbenes generally form an interesting group of molecules because of their conformational properties.[41-43] Assuming the mesogenic molecules is in *trans* conformation, the resulting effective transverse dipole moment μ_t is larger than the longitudinal μ_l. This results in the dielectric relaxation strength $\Delta\epsilon$ of the α process of 4-6-PMA, mainly asscociated with μ_t, stronger than that of the δ process mainly associated with μ_l;[35] see Figure 2a and Table II. The sample will exhibit a negative dielectric anisotropy $\epsilon_a \equiv \epsilon_\parallel' - \epsilon_\perp' < 0$ in the nematic phase and measuring frequency range, where $\epsilon_\parallel'$ and $\epsilon_\perp'$ are the dielectric constants when the nematic director in a monodomain is parallel to and perpendicular to the measuring electric field.

The isomeric effect on the δ and α processes is very obvious, i.e., 4-6-PMA shows both δ and α peaks (Figure 2a) while 4′-6-PMA shows only an α process (Figure 2b). Although both samples were measured under almost identical condition, a question can be raised about the macroscopic alignment states of the samples since the homeotropic alignment would cause an enhancement of the δ peaks and a suppression of the α peaks as compared with the unaligned state. On the other hand, the planar or homogeneous alignment would show just the opposite result.[24,25,27,34] In this sense, it seems that 4-6-PMA tends to be homeotropically aligned and 4′-6-PMA tends to be planarly aligned in the measuring dielectric cells. To verify this, an experiment regarding macroscopic alignment by a magnetic field has been conducted on the sample 4′-6-PMA, taking advantage of the dimagnetic anisotropy of "*trans*-methylstilbene". The sample was placed in an 8-T superconducting magnet (Cryomagnetics, Inc.) with either

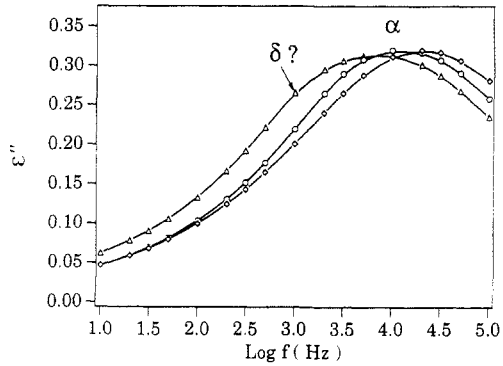

Figure 3. Dielectric loss spectrum of the sample 4′-6-PMA at 360 K in an 8-T magnetic field monitored by a CGA-83 bridge: △, homeotropic (H–) configuration; ◇, planar (P–, or homogeneous) configuration; ○, the sample in a zero magnetic field. Note, a dc conductivity of approximate 7.5×10^{-10} S/m has been extracted.

homeotropically or planarly mounting configuration, cooling slowly from well above isotropic temperature to room temperature. The cooling rate of 5 K/h was well controlled by a Lakeshore temperature controller together with a custom-built ramp circuit. For the homeotropic (H–) alignment, the sample cell was mounted with its layer normal parallel to the field; for the planar (P–, or homogeneous) alignment, the layer normal was perpendicular to the field. During each aligning process, the sample was monitored and recorded dielectrically by a CGA-83 bridge. The results are quite surprising as seen in Figure 3 for the sample at 360 K after a dc conductivity of approximate 7.5×10^{-10} S/m has been extracted. The strong magnetic field has little impact on the appearance of the relaxation process. The 4′-6-PMA with a planar cell has a spectrum similar to the unaligned sample while the sample with a homeotropic cell shows a slight rise of the δ peak. This δ appearance is still much weaker in comparison with 4-6-PMA even when 4′-6-PMA was subjected to an 8-T field! The macroscopic alignment texture after the magnetic field treatment has been confirmed with a Nikon polarizing microscope. While both samples have the same glass transition temperature (see Table I), the relaxation time of the 4′-6-PMA α process lies between those of the α and δ processes of 4-6-PMA at a given temperature (see Table II and Figure 4). This might partly result from an intermediate moment of inertia of the 4′-6-PMA mesogen compared with those associated with the α and δ processes of 4-6-PMA.

The effective dipole moments μ_t and μ_l may vary in terms of the position of methyl–CH_3 in the bridging group. For the 4-6-PMA sample, the resulting μ_t and μ_l are of same order of magnitude so that both α and δ processes are dielectrically active and observable. For 4′-6-PMA, the μ_t might be much larger than the μ_l, which results in hardly-observed δ process, mainly associated with the μ_l's reorientation. In this sense, the interpretation for the isomeric effect is similar to the results by Kresse *et al.*[37] However, their sample contains a siloxane backbone with no polar group and some very polar aromatic ester groups in the side chain. From the structures given in our sample, the backbone polymethacrylate has a polar ester group and the mesogenic stilbene in the side chain is not very

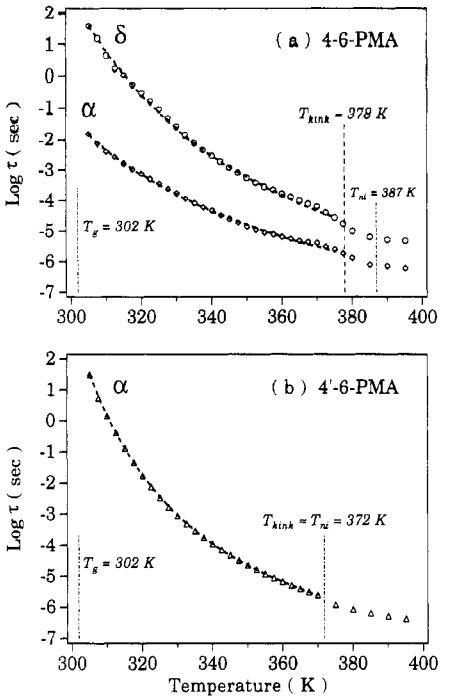

Figure 4. Relaxation time versus temperature: (a) 4-6-PMA, ○, δ process and ◇, α process; (b) 4'-6-PMA, only one process α (△) was observed. Dashed curves represent the Vogel–Fulcher–Tammann–Hesse (VFTH) fittings according to eq 8 in the temperature region below T_{kink}. T_g and T_{ni} are respectively glass transition and isotropic transition from DSC scan.

polar. In other words, the net contributions to the effective dipole moments respectively from the backbone and the side chain are comparable; i.e., the reorientation motion of the polar group in the polymer backbone may also involve the relaxation process. Hasse and co-workers have generalized the dielectric relaxation formula by adding a term to include isotropic reorientation of certain groups in the polymer backbone, irrespective of the macroscopic alignment.[26] Therefore, due to the possibility of both polymer backbone and side chain involved, the very small variance in relaxation amplitudes under an 8-T magnetic field might result from the macroscopic orientation of the mesogenic side chain on the *strong* background of the backbone chain. The isomeric effect of the mesogenic side chain on the packing formation of the polymer backbone nevertheless remains a puzzle. In short, the α process of 4'-6-PMA can virtually be thought of as a combination of two processes rather than a single α process in the original sense of rotational modes.

Activation Energy. The relaxation times obtained from HN data fitting versus temperature are shown in Figure 4. Overall, the relaxation time for each process decreases from approximately $10^{1.5}$ to $10^{-6.2}$ s as temperature increases from the glass transition ($T_g \approx 302$ K) to 400 K. There is a kink near nematic–isotropic transition T_{ni}. For 4-6-PMA, see Figure 4(a), the kink temperature T_{kink} for both α and δ processes is approximately 378 K, about 9 K below its T_{ni} = 372 K. For 4'-6-PMA (see Figure 4b), $T_{kink} \approx T_{ni}$ = 372 K. When the temperature goes above T_{kink}, each process appears to have an Arrhenius characteristic, i.e., activation energy E_A is independent of temperature. The Arrhenius expression is

$$\tau = \tau^\circ \exp\left(\frac{E_A}{RT}\right) \tag{7}$$

where τ° is a high-temperature limited relaxation time and R is the gas constant, 8.314 J/(K mol). The kink temperature T_{kink} is practically the nematic–isotropic transition T_{ni}, even though it sometimes differs from the T_{ni} obtained by DSC measurement. In the isotropic phase, where the nematic director field disappears, the activation energy E_A is approximately 36 and 37 kJ/mol, respectively for the δ process and α process of 4-6-PMA; $E_A \approx 56$ kJ/mol for 4'-6-PMA. The δ and α processes of 4-6-PMA have a very close activation energy, which is typical of the isotropic phase behavior. The fact that 4'-6-PMA has a higher activation energy in the isotropic phase than any of two processes of 4-6-PMA and is smaller than sum of them reflects, to some extent, that the 4'-6-PMA relaxation process is a combination of the two processes.

When both samples are in the nematic phase, $T_g < T < T_{kink}$, the relaxation times are strongly dependent upon temperature, especially when the temperature approaches T_g (see Figure 4), exhibiting a non-Arrhenius characteristic. The key concept for systematically synthesizing side-chain LCPs is an introduction of a flexible spacer between the liquid crystal mesogenic side group and the polymer backbone.[44,45] Although the spacer helps decouple the motion of the mesogenic group from the main chain and this decoupling becomes more effective with increasing spacer length, this kind of decoupling is nevertheless incomplete. Each relaxation process of the mesogens in nematic phase will still be influenced by the flexibility and motion of the polymer backbone, in particular, when the temperature approaches the glass transition from the nematic phase the relaxation times will be rising much faster than that indicated by an Arrhenius behavior (eq 7). As mentioned above, in this case, the reorientation of the polar group in the polymer backbone may make a significant contribution to the observed relaxation process. Based on free-volume theory,[46] this type of glassy behavior can be described by the Vogel–Fulcher–Tammann–Hesse (VFTH) equation[20]

$$\tau = \tau^\circ \exp\left(\frac{B}{T - T_\infty}\right) \tag{8}$$

where τ° is a short-limited relaxation time, in most cases, between 10^{-12} and 10^{-10} s, B is an activation parameter, T_∞ is called Vogel temperature or the ideal glass temperature, usually a few tens of degrees below T_g. The dashed curves in Figure 4 represent the VFTH fitting in the temperature range from T_g to T_{kink}, and the VFTH fitting parameters for each process are listed in Table III. The Vogel temperature T_∞ is 233.6 and 227.8 K, respectively, for the δ and α processes of 4-6-PMA and 269.6 K for 4'-6-PMA.

It is of interest that a general form of the effective activation energy for each process can be derived. From the Arrhenius expression in eq 7, one can have a generalized format for an activation energy

$$E_A = R\frac{\partial \ln \tau}{\partial(1/T)} \tag{9}$$

Because the samples are in nematic phase $T > T_g$, then $(T_\infty/T) < (T_g/T) < 1$, together with VFTH equation 8, we have

$$\frac{\partial \ln \tau}{\partial(1/T)} = B\frac{\partial}{\partial(1/T)}\left(\frac{1}{T - T_\infty}\right) = \frac{B}{(1 - T_\infty/T)^2} \tag{10}$$

Finally

$$E_A = \frac{RB}{(1 - T_\infty/T)^2} \tag{11}$$

It follows that the temperature dependence of an activation energy for any relaxation process can be expressed in terms of parameters B and the Vogel temperature T_∞ from the VFTH equation (8). Figure 5

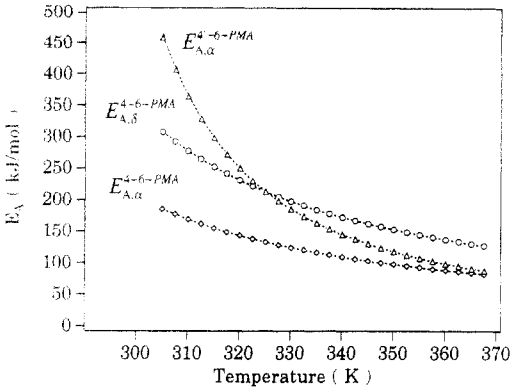

Figure 5. Activation energy from a general formula eq 11 composed of FVTH parameters: ○, δ process and ◇, α process of 4-6-PMA; △, α process of 4′-6-PMA.

Table III. Results from Vogel–Fulcher–Tamann–Hesse Equation (8) for the Two Major Processes of 4-6-PMA and 4′-6-PMA

	δ process			α process		
sample	τ^0 (10^{-10} s)	B (K)	T_∞ (K)	τ^0 (10^{-10} s)	B (K)	T_∞ (K)
4-6-PMA	0.191	2034	233.6	1.294	1435	227.8
4′-6-PMA				3.287	899.7	269.6

shows the activation energies versus temperature according to eq 11. The activation energy for the α process of 4′-6-PMA, $E_{A,\alpha}{}^{4'\text{-}6\text{-}PMA}$, lies between the α process $E_{A,\alpha}{}^{4\text{-}6\text{-}PMA}$ and the δ process $E_{A,\delta}{}^{4\text{-}6\text{-}PMA}$ of 4-6-PMA as long as the temperature is above 325 K. For 4-6-PMA, the *trans*-methylstilbene in the side chain can be treated as rigid-rod-like; it needs very large energy to overcome the nematic director field along the nematic direction (approximately along the long axis of the molecule) to be activated rotating about its short axis (δ process), while the rotation about its long axis associated with α process needs a relatively small activation energy. For 4′-6-PMA, basically only one α process of reorientation of the transverse dipole moment is prevailed in conjunction of the involvement of the polar group in the polymer backbone, which has an intermediate effective dipole moment coupling with a nematic field to form a localized potential that is roughly equivalent to an activation energy the molecule overcomes to perform the relaxation process. It is therefore very natural that $E_{A,\alpha}{}^{4\text{-}6\text{-}PMA} > E_{A,\alpha}{}^{4'\text{-}6\text{-}PMA} < E_{A,\delta}{}^{4\text{-}6\text{-}PMA}$ in the temperature range above 325 K. However, $E_{A,\alpha}{}^{4'\text{-}6\text{-}PMA}$ deviates in the region between $E_{A,\alpha}{}^{4\text{-}6\text{-}PMA}$ and $E_{A,\delta}{}^{4\text{-}6\text{-}PMA}$ when $T < 325$ K, and the $E_{A,\alpha}{}^{4'\text{-}6\text{-}PMA}$ increases rapidly as the temperature approaches T_g (see Figure 5). The cause of this complex activation process of the side group mesogens, with the glassy state of the polymer, remains unclear.

In the neighborhood of the kink temperature $T \leq T_{kink}$, $E_{A,\alpha}{}^{4\text{-}6\text{-}PMA} \approx 82.5$ kJ/mol, $E_{A,\delta}{}^{4\text{-}6\text{-}PMA} \approx 127.2$ kJ/mol, and $E_{A,\alpha}{}^{4'\text{-}6\text{-}PMA} \approx 87.2$ kJ/mol. The difference in activation energies at T_{kink}, $E_A{}^n - E_A{}^i$, may be related to the corresponding enthalpy change in DSC scan. The total $E_A{}^n - E_A{}^i$ for 4-6-PMA ($\alpha + \delta \approx 137$ kJ/mol) is much larger than that for 4′-6-PMA ($\alpha \approx 31$ kJ/mol), which is qualitatively consistent with the DSC measurement.[8,9]

Conclusion

From broad band frequency dielectric relaxation spectra, incorporated into the Havriliak–Negami dielectric empirical line shapes, there are two typical relaxation processes (low-frequency δ and high-frequency α) in a nematic liquid crystalline polymethacrylate containing a 4-methoxy-4′-hydroxy-α-methylstilbene mesogenic side group (4-6-PMA), while the corresponding polymethacrylate containing the constitutional isomeric mesogenic side chain (4′-6-PMA) hardly exhibits both δ and α processes even in a homeotropic cell subjected to an 8-T magnetic field. Both the mesogenic side chain and polar group in the polymer backbone may be involved in the relaxation process. A general formula for a temperature-dependent activation energy has been expressed in terms of Vogel–Fulcher–Tammann–Hesse parameters. The "kink" temperature in the relaxation time diagram is virtually at the nematic–isotropic transition point.

Acknowledgment. We are indebted to Professor V. Percec for providing the side-chain liquid crystalline polymer samples and motivated discussions. We benefited from many helpful discussions with Professor A. M. Jamieson, Professor C. Rosenblatt, and Dr. R. B. Akins. This work was supported by NSF Materials Research Group at Case Western Reserve University through Grant DMR 89-01845. Partial support for Z.Z.Z. by NSF/S&TC Advanced Liquid Crystalline Optical Materials (ALCOM) under Grant DMR 89-20147 is also gratefully acknowledged. The helpful comments made by the two reviewers are greatly appreciated.

References and Notes

(1) Finkelmann, H. *Philos. Trans. R. Soc. London, A* **1983**, *309*, 105.
(2) Ringsdorf, H.; Schneller, A. *Makromol. Chem., Rapid Commun.* **1982**, *3*, 557.
(3) Engel, M.; Hisgen, B.; Keller, R.; Kreuder, W.; Reck, B.; Ringsdorf, H.; Schmidt, H.-W.; Tschirner, P. *Pure Appl. Chem.* **1985**, *57*, 1009.
(4) Finkelmann, H.; Kiechle, U.; Rehage, G. *Mol. Cryst. Liq. Cryst.* **1983**, *94*, 343.
(5) Coles, H. J. *Faraday Discuss. Chem. Soc.* **1985**, *79*, paper 10.
(6) Coles, H. J.; Simon, R. In *Polymeric Liquid Crystals*; Blumstein, A., Ed.; Plenum Press: New York, 1985, p 351.
(7) Percec, V.; Tomazos, D. *Polymer* **1989**, *30*, 2124.
(8) Percec, V.; Tomazos, D. *Macromolecules* **1989**, *22*, 2062.
(9) Percec, V.; Tomazos, D.; Pugh, C. *Macromolecules* **1989**, *22*, 3259.
(10) Percec, V.; Tomazos, D. *J. Polym. Sci., Polym. Chem. Ed.* **1989**, *27*, 999.
(11) Percec, V.; Tomazos, D.; Wilingham, R. A. *Polym. Bull.* **1989**, *22*, 199.
(12) Silvestri, R. L.; Koenig, J. L. *Macromolecules* **1992**, *25*, 2341.
(13) (a) Gu, D.; Jamieson, A. M.; Rosenblatt, C.; Tomazos, D.; Lee, M.; Percec, V. *Macromolecules* **1991**, *24*, 2385. (b) Gu, D.; Jamieson, A. M.; Kawasumi, M.; Lee, M.; Percec, V. *Macromolecules* **1992**, *25*, 2151. (c) Gu, D.; Jamieson, A. M.; Lee, M.; Kawasumi, M.; Percec, V. *Liq. Cryst.* **1992**, *12*, 961. (d) Gu, D.; Smith, S. R.; Jamieson, A. M.; Lee, M.; Percec, V. Submitted for publication in *J. Phys. (Paris)*.
(14) (a) Maier, V. W.; Saupe, A. *Z. Naturforsch. A* **1959**, *14*, 882. (b) Maier, V. W.; Meier, G. *Z. Naturforsch. A* **1961**, *16*, 262. (c) Maier, V. W.; Saupe, A. *Z. Naturforsch. A* **1960**, *15*, 287. (d) Maier, V. W.; Saupe, A. *Mol. Cryst.* **1966**, *1*, 515.
(15) Nordio, P. L.; Rigatti, G.; Segre, U. *Mol. Phys.* **1973**, *25*, 129.
(16) Nordio, P. L.; Segre, U. In *The Molecular Physics of Liquid Crystals*; Luckhurst, G. R., Gray, G. W., Eds.; Academic Press: New York, 1979; p 411.
(17) Araki, K.; Attard, G. S.; Kozak, A.; Williams, G.; Gray, G. W.; Lacey, D.; Nestor, G. *J. Chem. Soc., Faraday Trans. 2* **1988**, *84*, 1067.
(18) Kozak, A.; Moscicki, J. K.; Williams, G. *Mol. Cryst. Liq. Cryst.* **1991**, *201*, 1.
(19) Zeller, H. R. *Phys. Rev. A* **1981**, *23*, 1434; *Phys. Rev. Lett.* **1982**, *48*, 334.
(20) Ngai, K. L.; Schönhals, A.; Schlosser, E. *Macromolecules* **1992**, *25*, 4915.
(21) Alig, I.; Kremer, F.; Fytas, G.; Roovers, J. *Macromolecules* **1992**, *25*, 5277.
(22) Zhong, Z. Z. Dielectric Relaxations in Side Chain Liquid Crystalline Polymers, Ph.D. Thesis; Case Western Reserve University, Cleveland, Ohio, 1993.

(23) McCrum, N. G.; Read, B. E.; Williams, G. *Anelastic and Dielectric Efforts in Polymeric Solids*; Dover Publications: New York, 1991; p 213.
(24) Attard, G. S.; Moura-Ramos, J. J.; Williams, G. *J. Polym. Sci., Polym. Phys. Ed.* **1987**, *25*, 1099.
(25) Williams, G.; Nazemi, A.; Karasz, F. E.; Hill, J. S.; Lacey, D.; Gray, G. W. *Macromolecules* **1991**, *24*, 5134.
(26) Bormuth, F. J.; Haase, *W. Liq. Cryst.* **1988**, *3*, 881.
(27) Haws, C. M.; Clark, M. G.; Attard, G. S. In *Side Chain Liquid Crystal Polymers*; McArdle, C. B., Ed.; Chapman and Hall: New York, 1989; p 196, and references cited therein.
(28) In practice, this is a technical problem while involving high frequency measurements. See ref 27, the side-chain LCP sample is generally treated as a capacitor C_p with a conductance G_p in parallel. It is essential above 10^5 Hz, and often convenient below, to model the leads (including the ITO electrodes in this paper) by introducing into the equivalent circuit an inductor L_s and a resistor R_s in series with the sample. The capacitance C and conductance G measured by the impedance analyzer in parallel mode are related to the equivalent circuit parameters by

$$\frac{G}{G^2 + \omega^2 C^2} = \frac{G_p}{G_p^2 + \omega^2 C_p^2} + R_s$$

$$\frac{C}{G^2 + \omega^2 C^2} = \frac{C_p}{G_p^2 + \omega^2 C_p^2} - L_s$$

(29) Havriliak, S.; Negami, S. *J. Polym. Sci.: Part C* **1966**, *No. 14*, 99.
(30) Cole, K. S.; Cole, R. H. *J. Chem. Phys.* **1941**, *9*, 341.
(31) Davidson, D. W.; Cole, R. H. *J. Chem. Phys.* **1950**, *18*, 1417; **1951**, *19*, 1484.
(32) Debye, P. *Ann. Physik.* **1921**, *39*, 789; *Polar Molecules*; Dover Publications: New York, 1945.
(33) Zhong, Z. Z.; Schuele, D. E.; Gordon, W. L.; Adamic, K. J.; Akins, R. B. *J. Polym. Sci., Polym. Phys. Ed.* **1992**, *30*, 1443.
(34) Zhong, Z. Z.; Gordon, W. L.; Schuele, D. E.; Akins, R. B.; Percec, V. *Mol. Cryst. Liq. Cryst.*, in press.
(35) Attard, S. G.; Araki, K.; Williams, G. *Br. Polym. J.* **1987**, *19*, 119.
(36) Kozak, A.; Moscicki, J. K. *Liq. Cryst.* **1992**, *12*, 377.
(37) Kresse, H.; Ernst, S.; Frücke, B.; Kremer, F.; Vallerien, S. U. *Liq. Cryst.* **1992**, *11*, 439.
(38) Klingbiel, R. T.; Genova, D. J.; Criswell, T. R.; Van Meter, J. P. *J. Am. Chem. Soc.* **1974**, *96*, 7651.
(39) De Jeu, W. H.; Lathouwers, Th. W. *Z. Naturforsch., A* **1975**, *30*, 79.
(40) Hedvig, P. *Dielectric Spectroscopy of Polymers*; John Wiley & Sons: New York, 1977; p 22.
(41) Mannfors, B. *J. Mol. Struct.* **1991**, *263*, 207.
(42) Ogawa, K.; Sano, T.; Yoshimura, S.; Takeuchi, Y.; Toriumi, K. *J. Am. Chem. Soc.* **1992**, *114*, 1041.
(43) Sension, R. J.; Szarka, A. Z.; Hochstrasser, R. M. *J. Chem. Phys.* **1992**, *97*, 5239.
(44) Percec, V.; Pugh, C. In *Side Chain Liquid Crystal Polymers*; McArdle, C. B., Ed.; Chapman and Hall: New York, 1989; p 30.
(45) Zhong, Z. Z.; Schuele, D. E.; Gordon, W. L. Submitted for publication in *Liq. Cryst.*
(46) McCrum, N. G.; Read, B. E.; Williams, G. *Anelastic and Dielectric Efforts in Polymeric Solids*; Dover Publications: New York, 1991; p 169.

Author Supplied Registry No. 4-6-PMA, 120416-97-9; 4′-6-PMA, 118400-13-8.